Available online at www.sciencedirect.com
ScienceDirect
Polymer 48 (2007) 3262–3272
polymer
www.elsevier.com/locate/polymer

Nanoencapsulation via interfacially confined reversible addition fragmentation transfer (RAFT) miniemulsion polymerization

Yingwu Luo*, Hongyan Gu

The State Key Laboratory of Chemical Engineering, Department of Chemical Engineering and Bio-Chemical Engineering, Zhejiang University, 38 ZheDa Road, Hangzhou, Zhejiang 310027, China

Received 1 December 2006; received in revised form 16 February 2007; accepted 7 March 2007
Available online 21 March 2007

Abstract

Oligomer of styrene and maleic anhydride synthesized by bulk RAFT polymerization (SMA-RAFT) was used to construct a novel strategy for robust nanoencapsulation via interfacially confined controlled/living radical miniemulsion polymerization. After ammonolysis, SMA-RAFT becomes amphiphilic and can be used as a surfactant to prepare miniemulsion. The ammonolyzed SMA-RAFT molecules would self-assemble on the interface of water/droplets. This self-assembly property combining with the RAFT living polymerization chemistry demands the polymer chains to grow inwards gradually in particles, leading to the formation of a polymer shell. The hydrophilicity of ammonolyzed SMA-RAFT agent tuned by the ammonolyzed degree or structures of SMA-RAFT agent was found to play a key role in the final morphology. The well-defined nanocapsules with little solid particles can be obtained by using partially ammonolyzed SMA-RAFT with 0.5 wt% SDS as a co-surfactant.

Keywords: Reversible addition/fragmentation transfer polymerization; Miniemulsion; Nanoencapsulation

1. Introduction

In the past decades, the research on the synthesis of polymeric nanocapsules has rapidly expanded. Nanocapsules of functional substances have shown promising applications in the area of drug delivery, catalysis, dye dispersion, optical medium, data storage, and so on. Compared with microencapsulation, the nanoencapsulation is more difficult in achieving integrated capsule morphology with well-controlled structural parameters like shell thickness and tunable shell functionalities. Many innovative techniques were reported. The layer-by-layer assembly of polyelectrolyte on nanoparticles showed an accurate and flexible control in shell thickness [1]. However, the technology is of low efficiency due to the tedious repeated layer-by-layer assembly processes. Nanoencapsulation based on the formation of micelles or capsules by block copolymer assembly in selective solvent is a simple process [2]. However, the process is carried out in a very dilute system (low efficient) and involves toxic organic solvent. Dendrimers have a high control over the size and shape and flexibility in surface and core functionalities [3], whereas the synthesis of dendrimer involves complicated many-step procedures such as repeated separation and reactions. Polymer brushes grafted from nanoparticles is another class of nanoencapsulation technique [4]. In such a case, the polymer chain grows out from the interior to the exterior.

In view of large-scale practical applications, a highly efficient and environmentally benign process is very much desirable. In this aspect, miniemulsion polymerization presents a promising technique for nanoencapsulation. Direct encapsulation of inorganic nanoparticles or carbon black was reported [5–7]. Encapsulation of small liquid organic substance was also reported [8–12]. In these cases, the encapsulation is provoked by phase separation during polymerization. Due to the strict thermodynamic and kinetic requirements, the encapsulation is very sensitive to the system parameters [8]. It is rather difficult

* Corresponding author. Tel.: +86 571 87951832; fax: +86 571 87951612.
E-mail address: yingwu.luo@cmsce.zju.edu.cn (Y. Luo).

0032-3861/$ - see front matter © 2007 Published by Elsevier Ltd.
doi:10.1016/j.polymer.2007.03.042

to obtain a well-defined core–shell structure. On the other hand, RAFT miniemulsion has been extensively investigated [13–24]. Monteiro et al. observed that core–shell nanoparticles of block copolymer could be formed in the seeded emulsion polymerization mediated by xanthate-based RAFT [25,26]. We have previously outlined a general strategy for nanoencapsulation of liquid substance by the interfacially confined RAFT miniemulsion polymerization [27]. The principle of the method is shown schematically in Fig. 1. An amphiphilic RAFT oligomer (SMA-RAFT agent for the current study) was designed and used as a surfactant to prepare miniemulsion (oil droplets of 50–500 nm dispersed in water). Due to their amphiphilic properties, SMA-RAFT molecules will self-assemble on the interface of water/droplets once miniemulsion is formed via ultrasonication. When a water-soluble initiator like potassium persulfate (KPS) is introduced, water-soluble primary radicals are born in water. After several additions of monomer, the oligoradicals become surface active and are captured by mini-droplets. The surface-active radicals with anionic head groups are anchored on the interface of mini-droplets and water. Since the SMA-RAFT agent molecules are also anchored on the interface, the radicals would transfer among the RAFT agents. By this way, the radical is located at the interface during most of the polymerization time, so the polymerization is confined on the interface. The polymer chains would grow inwards gradually, leading to the formation of a polymer shell.

To achieve an ideal nanoencapsulation via the RAFT interfacial miniemulsion polymerization, it is very much desirable to have the droplet nucleation to be the only particle formation mode. Since the RAFT agent also plays a role of surfactant, its molecular structure and hydrophilicity could exert a significant influence on the droplet size and droplet size distribution of the miniemulsion, which determine the efficiency of the droplet nucleation. So, the influence of the structures of SMA-RAFT and their hydrophilicities on nanoencapsulation is investigated in the present work. Adding external surfactant, as another approach to tune the droplet size and droplet size distribution, is also explored to optimize the encapsulation efficiency.

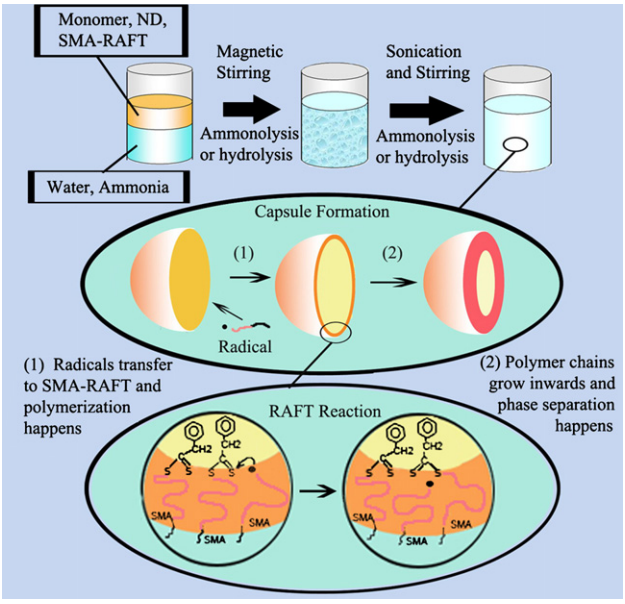

Fig. 1. Illustration of encapsulation principles by RAFT interfacial miniemulsion polymerization.

2. Experimental section

2.1. Materials

Styrene (St) was vacuum distilled before use. The RAFT agent, 1-phenylethyl phenyldithioacetate (PEPDTA), was synthesized according to the literature [28]. 2,2′-Azoisobutyronitrile (AIBN) was re-crystallized twice from methanol. Maleic anhydride (MAn, AR), sodium dodecyl sulfate (SDS, AR), *n*-nonadecane (ND, AR), and potassium persulfate (KPS, AR) were used as received. Ammonia aqueous solution was diluted to 5 wt% prior to use. For the miniemulsion polymerizations, de-ionized water was used.

2.2. Synthesis of SMA-RAFT agents

The co-oligomer RAFT agent of St and MAn was synthesized by the RAFT bulk copolymerization of St and MAn mediated by PEPDTA in a 60 °C water bath [29,30]. The molar ratio of [St]:[MAn]:[PEPDTA]:[AIBN] was 225:25:5:1. To study the influence of the SMA-RAFT structures on the encapsulation efficiency, a series of SMA-RAFT agents (SMA-RAFT1, SMA-RAFT2, SMA-RAFT3) were synthesized under the same experimental conditions but with different polymerization times. The products were discharged after 70 min, 100 min and 130 min of reaction, respectively. The resultant SMA-RAFT agents were collected by twice precipitation with methanol and dried under vacuum at 40 °C.

2.3. Miniemulsion preparation and polymerization

To prepare miniemulsion two types of procedures were used depending on different recipes. Procedure I: a solution of styrene (16 g, 0.15 mol), the SMA-RAFT agent (0.64 g, 0.45 mmol of SMA-RAFT1 in Run 2 for example), and the core material (ND, 4 g, 0.015 mol) was mixed with the water phase containing a certain amount of ammonia (0.22 g, 5 wt%, 0.65 mmol in Run 2 for example). After 20-min magnetic stirring (60 °C, Step 1), the mixture was applied to ultrasonication using an ultrasonic processor (KS-600) with 70% amplitude for 10 min in a 50 °C water bath (Step 2). During the ultrasonication process, the anhydride groups of the SMA-RAFT agent were ammonolyzed in the interface of oil and water [31,32]. The ammonolyzed SMA-RAFT agent would become amphiphilic and stabilize the miniemulsion. Then the miniemulsion was allowed for another 60 min for further ammonolysis or hydrolysis under magnetic stirring at 60 °C (Step 3). The dispersion was then ultrasonicated for another 15 min at 50 °C to form the final miniemulsion (Step 4). The final miniemulsion was then transferred to a round-bottomed flask. After 30-min nitrogen purge, the miniemulsion polymerization was

started up via the injection of a potassium persulfate aqueous solution (0.16 g, 0.59 mmol in 5 g of water). The polymerization temperature was 68 °C. The reaction was carried on for 5 h to reach a conversion over 90%. For Procedure II, Steps 2 and 3 were not implemented. Procedure II (single sonication) is simpler than Procedure I (sonication–ammonolysis–sonication). However, the latter was expected to lead to the miniemulsion with smaller droplet size and narrower droplet size distribution.

The recipe and preparation procedure of the miniemulsion for all experimental runs are summarized in Table 1.

2.4. Surface tension

Surface tensions of miniemulsions were measured on a video-based contact angle measuring device (OCA20, DataPhysics Inc.). Hanging drops of miniemulsion were extruded through a needle tube ($\Phi = 2.41$ mm, at room temperature) to measure the surface tension. Every value was statistically evaluated by repeated monitoring for not less than 15 times.

2.5. pH value detection

The pH values of the emulsion were detected by a pH-meter (LEICI PHS-2C). The electrode type was E201-4.

2.6. GPC analysis

Samples were taken during polymerization and the process was inhibited by adding a dose of hydroquinone solution (0.3% in ethanol). The samples were dried in a vacuum oven at 200 °C for 6 h to evaporate water, ND, and residual monomer. Molecular weight and molecular weight distribution of the polymeric shell of particles and SMA-RAFT were characterized by GPC (Waters150). Molecular weights were derived from a calibration curve based on polystyrene standards. For the shell polymer measurements, Waters Styragel Columns HR 4, 3, 2 (the calibration range: 1000–70000 g/mol) were used. For the SMA-RAFT agent characterization, Waters Styragel Columns HR 3, 2, 1 (the calibration range: 20–20000 g/mol) were used. The effluent was tetrahydrofuran with a flow rate of 1.0 ml/min.

Table 1
Recipe and preparation procedures of the miniemulsion

Run	1	2	3	4	5	6	7	8	9
St:$C_{19}H_{40}$ (wt)	4:1	4:1	4:1	4:1	4:1	4:1	4:1	1:1	4:1
SDS[a] (wt%)	0	0	0	0	0	0	0.5	0.5	0.5
SMA-RAFT1[b] (mol%)	0.30	0.30	0.30	0.30	0	0	0.3	0	0
SMA-RAFT2[b] (mol%)	0	0	0	0	0.30	0	0	0.2	0
SMA-RAFT3[b] (mol%)	0	0	0	0	0	0.37	0	0	0.2
KPS[b] (mol%)	0.38	0.38	0.38	0.38	0.38	0.38	0.38	0.38	0.38
NH_3:MAn (mol)	1:3	1:3	0.9:1	2:1	2:1	2:1	1:3	1:3	1:3
Procedure	II	I	I	I	I	I	II	II	II
Solid content (wt%)	20%	20%	20%	20%	20%	20%	20%	20%	20%

[a] The weight percentage of SDS was based on the oil phase.
[b] The molar percentage of SMA-RAFT and KPS was based on the monomer.

2.7. Encapsulation efficiency analysis

The fraction of encapsulated particles was determined by dividing the encapsulated particle number by the total particle number, counted from TEM images. Every statistical number was calculated from not less than 500 particles.

2.8. Particle size measurement

The particle size and its distribution were measured by Malvern ZETASIZER 3000 HAS.

2.9. Particle morphology observations

Transmission electron microscopic measurement was performed on a JEOL JEM-1230 transmission electron microscope at 80 kV. The latex of miniemulsion was diluted to 0.03 wt%, mounted on 400-mesh carbon-coated copper grids, and dried in an oven at 40 °C. Little ND evaporated during drying.

3. Results and discussion

3.1. St/MAn RAFT copolymerization

The RAFT copolymerization of St with MAn exhibits some interesting features. MAn does not homo-polymerize, and its copolymerization with St has a strong tendency toward alternation, indicated by the reported reactivity ratios (0.02 for St and 0 for MAn) [33,34]. Such a feature was used to synthesize block copolymer of poly(St/MAn-*b*-St) by one pot RAFT polymerization [29,30,35–38]. In the first stage of polymerization before MAn is consumed, the resultant polymer chains are poly(St-*alt*-MAn), which can further be converted into hydrophilic segments. In the second stage of polymerization when MAn is exhausted, the extended chains are composed of PS homo-polymer segment, which is hydrophobic. So, simply by controlling the reaction time, we synthesized SMA-RAFT agents with different chain lengths and varied amphiphilic properties.

The composition profile along SMA-RAFT polymer chains under the current synthesis conditions can be calculated by Monte Carlo simulation with penultimate model using parameters reported by Hill et al. [39]. The calculated diad fractions for the current polymerization conditions are presented in Fig. 2. For a strict alternative microstructure, the fraction of SMA diad should be unit and the fraction of SS should be zero. From Fig. 2, it is derived that the chain microstructure is very close to an alternative structure before DP reaches 12. After DP = 20, the homo-polystyrene block would be formed. Between DP = 12 and 20, the fraction of diad SS dramatically increases. It should be pointed out that the saw-like curve before DP = 12 is not caused by the calculated error but due to the reactivity ratios. Since MAn cannot homo-polymerize at all, once a SMA diad is formed, the next added monomer

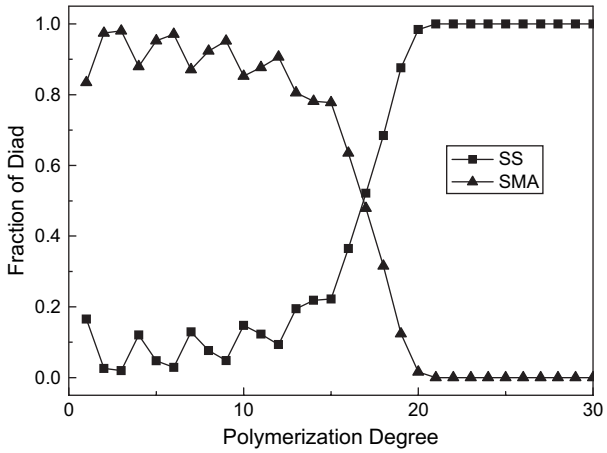

Fig. 2. The chain microstructures of SMA-RAFT agents versus polymerization degree.

must be styrene. On the other hand, styrene can be homopolymerized. That means that it is still possible for styrene to add to a styrene radical. The different alternative propagation preference of styrene and MAn radicals leads to the saw-like curve shown in Fig. 2.

The molecular weight and its distribution of three SMA-RAFT agents synthesized in this work are listed in Table 2. From Table 2 and Fig. 2, it is estimated that SMA-RAFT1 is composed only of the hydrophilic segment with 4.5 units of MAn and 6.9 units of St on average. The average styrene composition is around 0.685. The degree of polymerization of SMA-RAFT2 was extended to around 15. The average styrene composition of the block from DP = 10 to 15 was estimated to be 0.733. As the degree of polymerization is increased further from 15, the fraction of SS diad dramatically increases due to the consumption of MAn. The average composition of the block from DP = 10 to 18 is 0.813. So, the hydrophilicity of three RAFT agents decreases in the order of SMA-RAFT3 (DP = 17.7) < SMA-RAFT2 < SMA-RAFT1.

3.2. The influence of the hydrophilicity of SMA-RAFT without co-surfactant

The synthesized SMA-RAFT agents are quite hydrophobic. The anhydride groups incorporated in the oligomer chains can

Table 2
Structural parameters of SMA-RAFT agents

Type	Conversion[a] (%)	$\overline{M}_n$[b] (g/mol)	DP[c]	PDI[b]
SMA-RAFT1	22.3	1414	11.4	1.12
SMA-RAFT2	30.1	1795	15.2	1.11
SMA-RAFT3	38.2	2037	17.7	1.12

[a] Determined by gravimetric method.
[b] Determined by GPC.
[c] Calculated by simulation.

be easily converted into much more hydrophilic groups via ammonolysis or hydrolysis. The ammonolysis process of SMA-RAFT could be described as in Scheme 1 [40,41]. Depending on the molar ratios of ammonia/anhydride units, anhydride groups of the SMA-RAFT agent could be ammonolyzed or hydrolyzed into different hydrophilic groups. When the molar amount of ammonia is less than that of the anhydride groups in SMA-RAFT, some of the anhydride groups are ammonolyzed according to Reaction (2), others could be further hydrolyzed as in Reaction (1). When the molar number of ammonia is more than that of anhydride groups, Reaction (3) would occur. All three reactions increase the hydrophilicity of the oligomer chains. For the current system, the ammonolysis was confirmed by FT-IR analysis [27].

SMA-RAFT1 is mainly composed of St/MAn *alt*-copolymer. The SMA-RAFT1 could be tuned from being quite hydrophobic to hydrophilic by manipulating the ammonolysis degree. A set of experimental runs (Runs 1–4) were designed to investigate the influence of the ammonolysis degree of SMA-RAFT1. The recipe and emulsification procedures are referred in Table 1. The pH values, which are used to monitor the ammonolyzing process, are listed in Table 3. The TEM images of the final latex are presented in Fig. 3.

In Run 1, the molar ratio of ammonia to anhydride groups was set to 1:3. The SMA-RAFT was partially ammonolyzed under such conditions. Procedure II was applied. From Table 3, it is seen that after emulsification by magnetic stirring, the system was still basic. But after 15-min sonication, the system became acidic, indicating that ammonia was exhausted. The gradual decrease in pH value during polymerization is partly because of the formation of H^+ during the decomposition of KPS. The anhydride groups left after ammonolysis

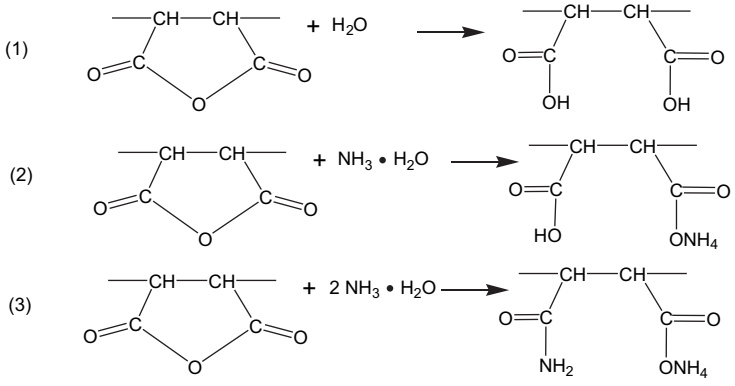

Scheme 1. The hydrolysis and ammonolysis process of SMA-RAFT agents.

Table 3
pH values at various stages of nanocapsule preparation

Run	Stage					
	Ammonia	Step 1 finished	Step 2 finished	Step 3 finished	Step 4 finished	Final latex
1	10.22	8.84	–	–	6.04	3.59
2	10.10	8.76	6.10	5.84	5.46	3.38
3	10.65	8.85	6.75	6.50	6.10	4.85
4	10.86	6.83	7.83	7.20	7.30	6.85

could be hydrolyzed during polymerization, which also contributes to the decrease in pH value.

The resultant particle morphology of the latex is shown in Fig. 3A. The dark part of the particles is PS polymer and the light part is ND. From the TEM pictures, it is seen that most of the particles appear to be solid, and a certain part of them is as small as 30–50 nm, others are around 100 nm, some are as large as 200 nm. The percentage of nanocapsules was counted to be only about 10 in number, and most of the capsules are about 180–240 nm in size and have a very thin shell. The weight ratio of core material to shell polymer is about 1:2 on average ($\rho_{polymer} = 1.08$ g/cm^3, $\rho_{ND} = 0.8$ g/cm^3), while the designed ratio is 1:4. It is likely that some 'pure' ND droplets, which could not be observed by TEM, existed in the final latex. These pure ND droplets might be derived from those very large droplets in the original miniemulsion. Due to the large size, the polymerization rate in those very large droplets could be much lower than that of those particles with much smaller size. In the final latex, the very large droplets could be converted into the 'pure' ND droplets with little polymer, the monomer of which is transported to other particles during polymerization.

As nonadecane is a super hydrophobic compound, it is hardly transferable among particles via the aqueous phase. From the large capsules ranging from 180 nm to 240 nm (the number average core diameter is 145 nm), it can be statistically estimated that the original droplet size prior to polymerization is about 230 nm on average. It means that about 50% of the monomer of these particles had been lost during polymerization. This might be ascribed to the poor surface activity of SMA-RAFT1, which was not suitable for making a fine miniemulsion. As a result, the formed miniemulsion would have a quite large droplet size as large as 230 nm, as estimated. Under such a condition, homogeneous nucleation might occur, leading to the formation of the solid particles. A lot of monomer would transfer from monomer droplets to those homogeneous nucleated particles (solid particles). Considering that the molecular weight distribution is monopeak as seen in Fig. 4, it is derived that the polymerization in those solid particles is also mediated by RAFT. It is possible that SMA-RAFT1 could be transported among particles in the early stage of polymerization, as supported by the surface tension data from Runs 2 and 4, which will be discussed later.

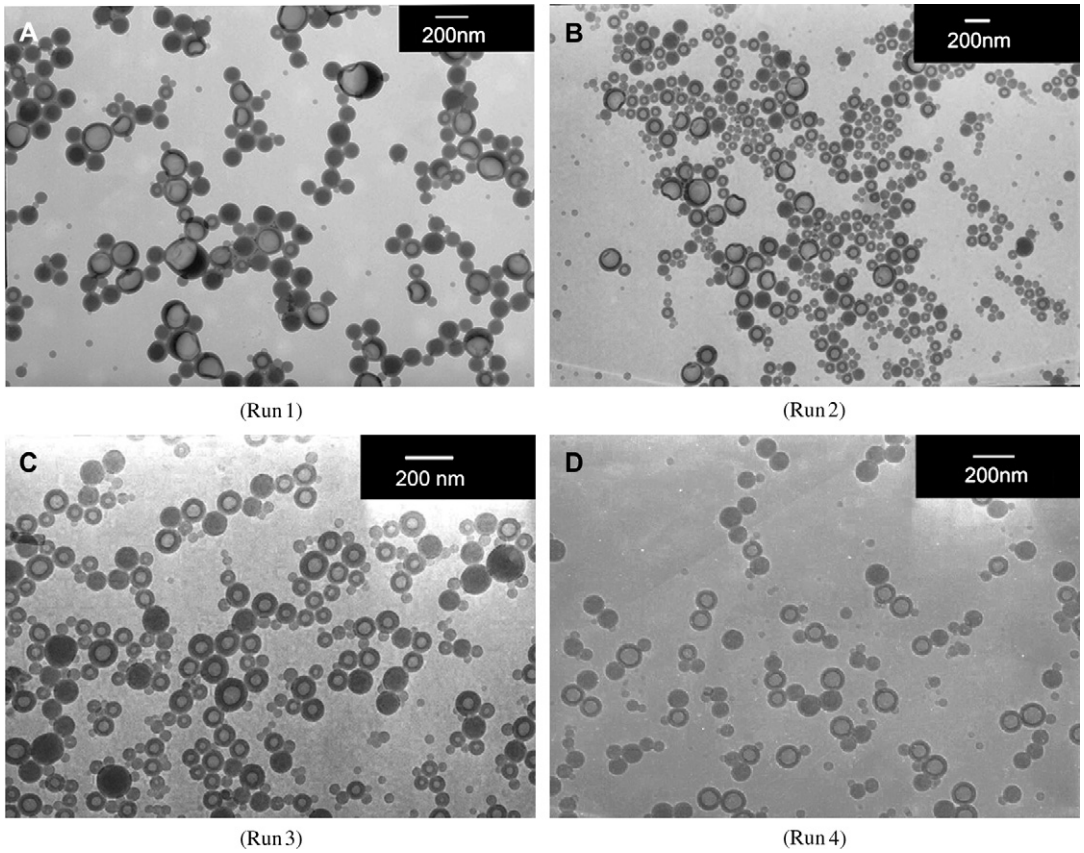

Fig. 3. TEM images of particles prepared by SMA-RAFT1, Runs 1–4.

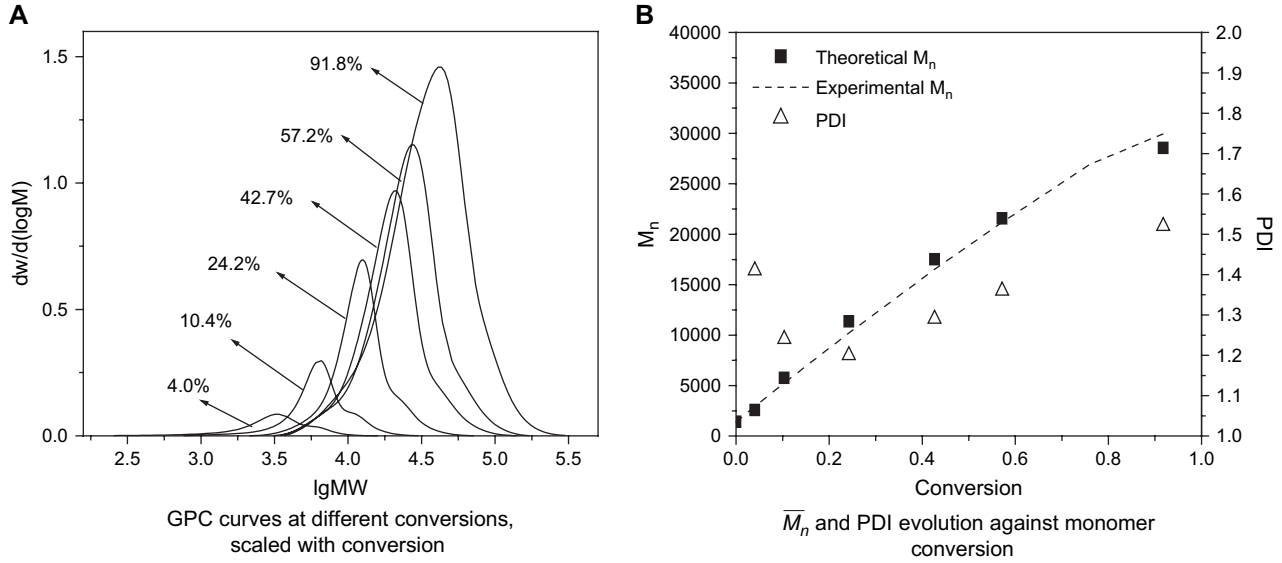

Fig. 4. Molecular weight and molecular weight distribution evolution against conversion of Run 2.

Run 2 involved a twice sonication operation (Procedure I). The twice ultrasonication operation not only accelerates the ammonolysis process, but also increases the hydrolysis degree of maleic anhydride units. The resultant monomer droplets were expected to be smaller. Thus, the homogeneous nucleation was expected to be suppressed. The pH values used during this experiment are listed in Table 3. It is seen that after the first ultrasonication process (Step 2), the pH value of the system is about 6.1. After further treatments, the pH value further decreases to 5.46, indicating that some of MAn units incorporated in SMA-RAFT1 are hydrolyzed. In fact, the ammonolysis/hydrolysis of SMA-RAFT1 and the emulsification intensify each other. The emulsification increases the interface area of oil–water, so that the SMA-RAFT molecules can get more chances to react with ammonia. At the same time, the ammonolyzed/hydrolyzed SMA-RAFT agents stabilize the newly formed monomer droplets.

Judged from the TEM pictures of the resultant latex (Fig. 3B), the encapsulation ratio of this attempt was improved largely compared with the results got from Procedure II. The encapsulation efficiency is about 50% in number. But it is found that the capsule size is still not uniform. Those particles with larger sizes have a higher core/shell ratio, which is about 1.5:1, but the core/shell ratio of smaller ones is 1:14 or even less. Only a very small fraction of particles have the core/shell ratio close to the set value of 1:4. According to the core size in the capsules of 180–240 nm (averagely 137 nm in number), the original droplet size prior to polymerization corresponding to these particles is estimated to be about 218 nm on average. It is inferred that although the ammonolysis procedure was extended, the resultant SMA-RAFT1 agent is still not sufficiently surface active and the monomer droplet size prior to polymerization is still not uniform. Those larger droplets would lose monomer during polymerization due to the weaker compartmentalization effect. Still, there are a fraction of solid particles generated in the system, most of which are about 20–30 nm in diameter.

By GPC, the molecular weight growth during polymerization was followed. As shown in Fig. 4A, the high molecular weight side of GPC curves moves faster than that of low molecular weight side with increase of monomer conversion in the late stage of polymerization. Molecular weight grows linearly with monomer conversion. The polydispersity index (PDI) remains below 1.55. For RAFT polymerization, the theoretical molecular weight can be calculated by [17,19]:

$$M_{n,th} = m_{RAFT} + \frac{[M]_0 m_{styrene} x}{[RAFT]_0 + f[I]_0(1 - e^{-k_d t})} \quad (1)$$

where m_{RAFT} is the molar mass of the RAFT agent, $m_{styrene}$ is the molar mass of styrene, x is the fractional monomer conversion, $[M]_0$ is the initial monomer concentration, $[RAFT]_0$ is the initial RAFT agent concentration, $[I]_0$ is the initial initiator concentration, k_d is the decomposition rate coefficient of the initiator, and t is the reaction time. f is the initiation efficiency, which is estimated to be 0.54 using the model proposed by Maxwell et al. [42]. The relevant parameter values used here are obtained from Refs. [24,42–46]. It should be noted that the concentrations of $[M]_0$, $[RAFT]_0$ in this expression are with respect to the *total organic phase but* $[I]_0$ *with respect to the aqueous phase*. It was reported that RAFT end groups could be hydrolyzed at basic conditions [47,48] and be oxidized by peroxide initiator [49].

In the current system, the hydrolysis of RAFT agent is likely to occur during the ammonolysis procedure. After the polymer chains in particles grow inward, the possibility of the hydrolysis of RAFT groups dramatically decreases because they are located in the particles. Oxidation is likely to occur only within a short time period after the injection of KPS. To take these side reactions into consideration, a modified factor of RAFT concentration is introduced accounting for the possible ineffectiveness of a fraction of RAFT agent during the ammonolysis. So, the theoretical molecular weight was calculated by:

$$M_{n,th} = m_{RAFT} + \frac{[M]_0 m_{styrene} x}{f_1[RAFT]_0 + f[I]_0(1 - e^{-k_d t})} \quad (2)$$

where f_1 is the modified factor.

From Fig. 4B, it can be seen that the molecular weight development is in good agreement with the theoretical expectation with $f_1 = 0.92$. It seems that only a small fraction of RAFT agent undergoes side reactions like hydrolysis of dithioester under alkaline conditions [47,48]. The PDI of the resultant polymer decreases firstly as expected for RAFT polymerization, and then backs up lately during polymerization. As discussed later, such an increase in PDI might not be ascribed to the irreversible termination but to the heterogeneous nature of the polymerization, as seen in RAFT miniemulsion polymerization [16].

In Run 3, the molar ratio of ammonia/anhydride units was increased to 0.9. In this case, the anhydride groups could be more sufficiently ammonolyzed, hence the hydrophilicity of the SMA-RAFT1 is increased. Correspondingly, pH values in the corresponding stages are larger (refer to Table 3). More anhydride groups were ammonolyzed.

From the TEM images of the final latex (Fig. 3C), it is seen that the uniformity of the particles and the encapsulation efficiency are significantly improved. The encapsulation ratio achieves about 60% in number. The capsules larger than 150 nm can hardly be observed, and the number average size of the capsules is about 75 nm. Furthermore, the capsules look more symmetric and the core/shell ratio is more close to the feed ratio of ND/St. It is concluded that increasing the hydrophilicity of the amphiphilic RAFT agent is crucial to suppress the homogeneous nucleation and monomer transportation among particles during polymerization and thus to obtain a well-defined capsule morphology.

However, besides the absence of large capsules over 150 nm, the solid particles are of bimodal distribution with a dominant fraction in the range of 80–110 nm and only a few fraction in about 20–40 nm.

From the GPC data in Fig. 5, it is seen that when the conversion is higher than 70%, the low molecular weight side of GPC curves stops growing with conversion. GPC with UV and RI dual detectors was used to check if the dithioester groups still existed in this section. Wavelength of UV was set to 311 nm, which is the feature absorbing peak of the dithioester groups [48,50]. UV and RI signals are compared in Fig. 6. From Fig. 6, it is clear that most of the chains in the low molecular weight side of GPC curves are still with the dithioester groups. The observation that the low molecular weight side of GPC curves stops growing with conversion during the high conversion range might be ascribed to the heterogeneous nature of the RAFT miniemulsion polymerization, as thoroughly discussed in Ref. [51]. The PDI of the resultant polymer is below 1.55. But the efficiency of the SMA-RAFT1 agent decreases to 0.84, indicating a larger loss of SMA-RAFT agent during the emulsification compared with the cases where less ammonia was applied.

In Run 4, the molar ratio of ammonia/anhydride groups was further increased to 2:1. To minimize the decomposition of the RAFT agent under such a basic condition, ammonia was added twice. The first dosage of ammonia was 0.75 g (5 wt%, NH_3:anhydride units = 1.1:1, added to water phase prior to emulsification) and the second dose of 0.6 g (5 wt%, NH_3: anhydride units = 0.9:1) was added between Steps 3 and 4 in the emulsification Procedure I. After the second sonication, the pH value of the system is 7.30 (see Table 3).

As indicated by the pH values after sonication (see Table 3), all anhydride groups are supposed to be fully ammonolyzed before polymerization. From the TEM pictures of the experiment (Fig. 3D), it is calculated that the encapsulation efficiency is much lower than in the case when NH_3:MAn = 0.9:1 (see Fig. 3C). However, the nanocapsules are uniform in size and shell thickness with an average size of 87 nm. The core/shell volume ratio is about 1:3 on average, indicating some of the monomer should have been lost during polymerization. This phenomenon is quite different from the case in Fig. 3A, where the core/shell ratio is about 1:7, though the encapsulation ratio

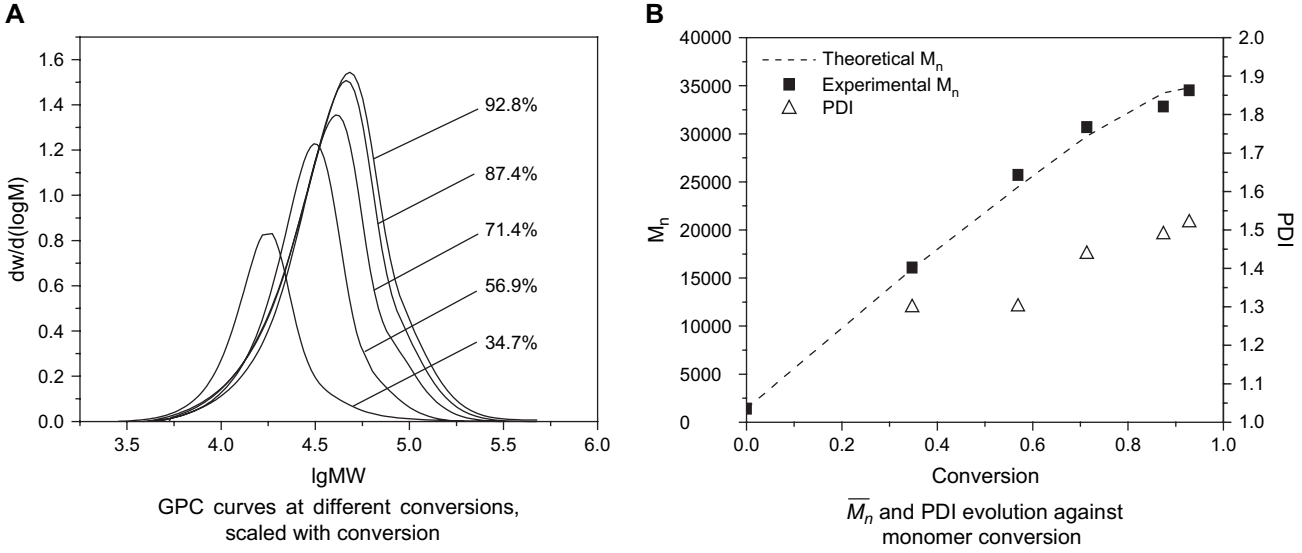

Fig. 5. Molecular weight and molecular weight distribution evolution against conversion of Run 3.

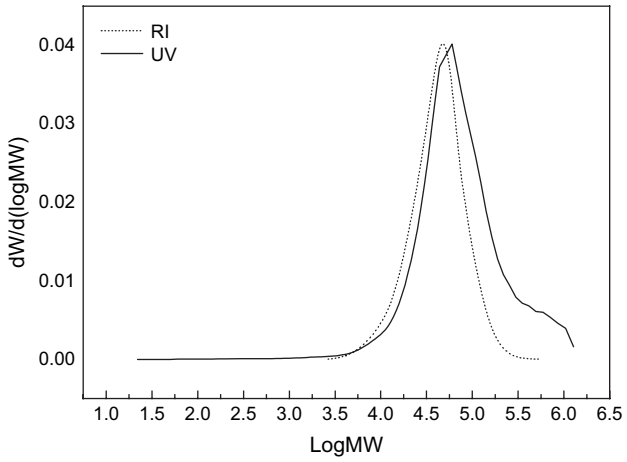

Fig. 6. The comparison of GPC curves from RI and UV, the final sample of Run 3.

is also quite low (about 30% in number). Similar to the case in Fig. 3C, the solid particles have a bimodal distribution of 100 nm and 30 nm in diameter.

GPC data were similar to that of Run 3, but the calculated efficiency of SMA-RAFT was only 0.79. PDI exceeded 1.6 at the end of polymerization. Although the pH value of the emulsion was controlled by twice addition of ammonia to avoid a severe basic condition, a little more fraction of the RAFT agent was still decomposed.

It was measured that the surface tension of miniemulsion prior to polymerization is 56.37 mN/m when NH_3:MAn = 1:3 in mole (pH: 5.30, 22 ± 0.2 °C, Run 2), and 55.54 mN/m when NH_3:MAn = 2:1 in mole (pH: 7.16, 22 ± 0.2 °C, Run 4). Considering that the surface tension of pure water is 73.38 mN/m, it can be estimated that there are a certain fraction of ammonolyzed SMA-RAFT1 dissolved in the aqueous phase. These RAFT agents dissolved in the water phase could react with the radicals in the water phase and stabilize the particles formed via the homogeneous nucleation. Thus, the homogeneous nucleation was likely to occur in these cases. Due to higher degree of ammonolysis in Run 4 than in Run 3, more SMA-RAFT1 molecules of the former would dissolve in the water phase, increasing the probability of the homogeneous nucleation. This might explain why Run 4 is worse in the encapsulation efficiency than Run 3.

3.3. The influence of SMA-RAFT structures

Two other SMA-RAFT agents with longer chain length (SMA-RAFT2, SMA-RAFT3, Run 5 and Run 6, respectively) were explored. As discussed previously, the hydrophobicity increases from SMA-RAFT1, SMA-RAFT2, to SMA-RAFT3. The ammonia molar amount for ammonolysis was set to be twice that of the anhydride groups, and twice ultrasonication (Procedure I) was used. Under these conditions, the anhydride groups incorporated in SMA-RAFT are supposed to be fully ammonolyzed to reach a maximum available hydrophilicity. The typical TEM images of the final latex obtained from these two RAFT agents are presented in Fig. 7.

From TEM images (Fig. 7A), it is found that the latex from SMA-RAFT2 has high encapsulation efficiency (60% in number) and the smaller solid particles (20–30 nm) are much less. The improvement of encapsulation efficiency indicates that by increasing the molecular weight of the SMA-RAFT agent, the homogeneous nucleation could be largely suppressed and the interfacial activity of the RAFT agent could be remained via full ammonolysis of SMA-RAFT2. The surface tension of the miniemulsion was found to remain almost the same and to be very close to that of pure water (see Table 4) during the whole polymerization process, which indicate that SMA-RAFT2 is scarcely dissolved in water.

When SMA-RAFT3 with more hydrophobicity was applied (Run 6), the resultant particle morphology is shown as in Fig. 7B. The encapsulation fraction is 0.36 in number, which is better than in the case of SMA-RAFT1 at the same ammonolyzed degree (Run 4), but inferior to that of SMA-RAFT2

Table 4
The surface tension of the miniemulsion during polymerization of Run 5

No.[a]	0	1	2	3	4	5
Surface tension (mN/m)	73.91	73.06	73.61	72.86	74.09	73.67

[a] The sample numbered 0 was taken before the addition of KPS, and samples 1–5 were taken at the conversion of 18.3%, 41.2%, 67.3%, 85.3% and 94.8% separately. Measured at 14 °C.

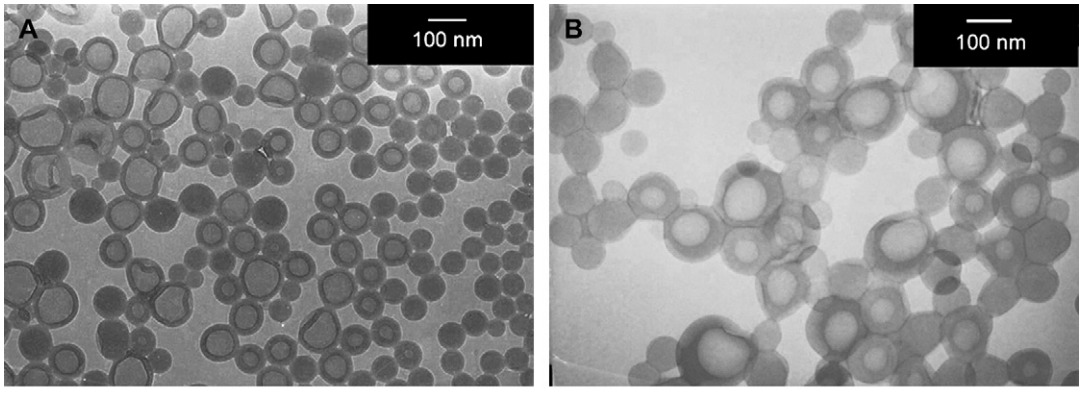

(SMA-RAFT2) (SMA-RAFT3)

Fig. 7. TEM images of particles synthesized by miniemulsion polymerization with different SMA-RAFT agents.

(Run 5). The particle size is 142 nm on average, which is larger than those of the other two cases. It is likely that SMA-RAFT3 is less effective in decreasing the oil–water interfacial tension than SMA-RAFT2 does due to more hydrophobicity. It is also likely that the viscosity of oil phase is higher than that of SMA-RAFT2 due to the higher molecular weight and weight concentration of SMA-RAFT3 in the oil phase. As a result, the droplet size of the miniemulsion using SMA-RAFT3 could be larger than that using SMA-RAFT2 [52], increasing the probability of the homogeneous nucleation.

The GPC curves of Run 6 look similar to Fig. 5. GPC data show that molecular weight grows in good agreement with the theoretical predications with a RAFT efficiency of 0.9, indicating that the SMA-RAFT3 agent has a higher stability against ammonia degradation during the emulsification compared with SMA-RAFT1. With increase in the length of the polystyrene hydrophobic segment, the dithioester groups become less accessible for ammonia due to that the dithioester groups are connected to the hydrophobic segment.

3.4. The influence of SDS as a co-surfactant

In the previous experiments, SMA-RAFT agents played a dual role of surfactant and RAFT agent. In order to achieve a high interfacial activity, a high degree of ammonolysis is desirable. However, this high degree of ammonolysis might be related to the formation of solid particles by enhancing the homogeneous nucleation, as inferred from the experimental data of Run 4. In the following set of experiments (Runs 7–9, refer to Table 1), another strategy was used. The degree of ammonolysis was controlled to be rather low. A co-surfactant (SDS) was applied to assist the emulsification. The typical TEM images of the final latex are presented in Fig. 8.

In Run 7, the dosage of ammonia was 1/3 in mole that of the anhydride groups in SMA-RAFT1. SDS level was 0.5 wt% of the oil phase. The miniemulsion was made with Procedure II. The TEM picture of the resultant latex is shown in Fig. 8A. Interestingly, the addition of SDS significantly improves the encapsulation efficiency. The number fraction of the encapsulating particles is over 0.8. The solid particles are so small that their volume fraction is actually less than 0.02. Furthermore, the core/shell ratio becomes quite close to the designed value and the particle size is rather uniform in 90 nm. The capsules look symmetric. Lowering the ammonolysis degree of SMA-RAFT1 would reduce the concentration of ammonolyzed SMA-RAFT in water. Therefore, the possibility of the homogeneous nucleation, which is assumed to be the main cause for forming the solid particles, is reduced. On the other hand, the addition of SDS also helps to decrease the droplet size. The monomer droplet nucleation becomes the main mechanism for particle nucleation as desired.

In the case of SDS/SMA-RAFT2 (Run 8), well-defined nanocapsules were also obtained. As seen from Fig. 8B, the core/shell ratio is 1:1 as designed but the polymer shell seems

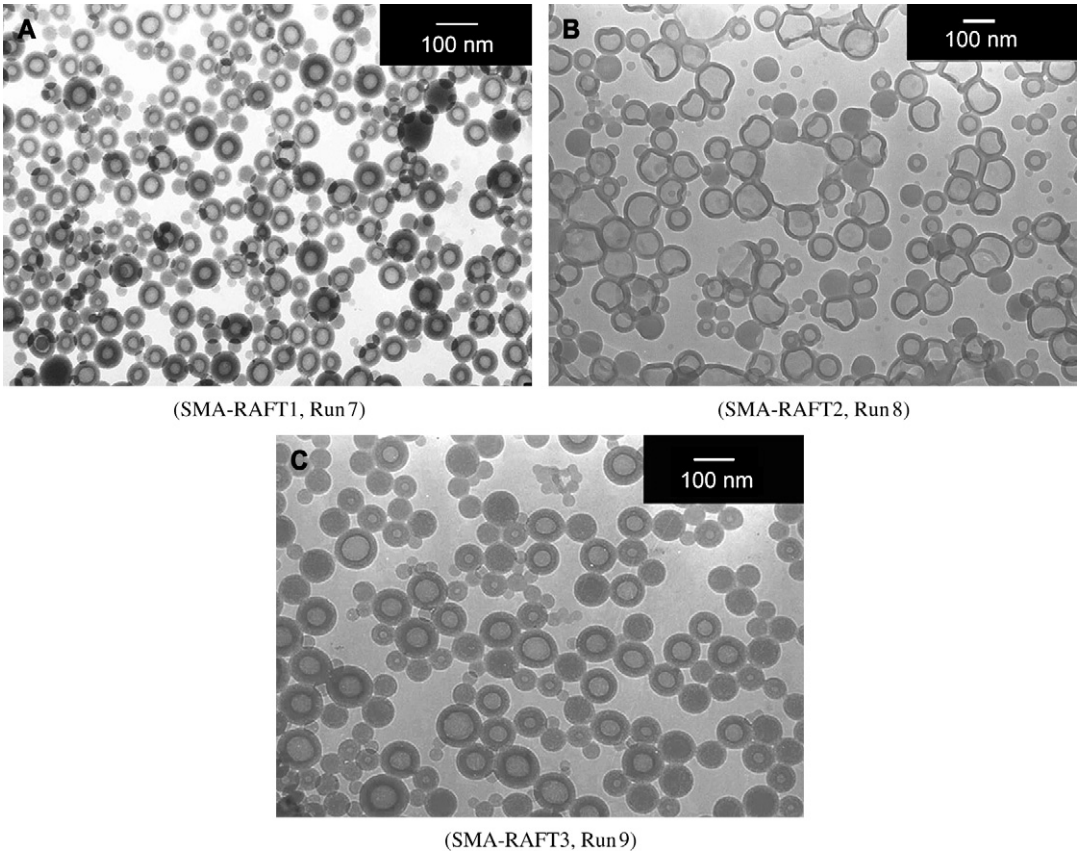

(SMA-RAFT1, Run 7) (SMA-RAFT2, Run 8)

(SMA-RAFT3, Run 9)

Fig. 8. TEM images of nanocapsules synthesized with SDS as a co-surfactant.

to be too thin to support the liquid core material with a sphere shape under TEM vacuum. The shell thickness appears uniform. The result also demonstrates that a large volume of core material is possible.

In Run 9, capsules with well-defined core–shell morphologies were also obtained, as evident from Fig. 8C. Compared with the case without SDS (Fig. 7B), the application of SDS clearly improves the capsule morphology. However, it is quite unexpected that some solid particles can still be seen in this case. It is possible there is the other mechanism to form the solid particles other than the homogeneous nucleation, which is worth further investigating.

4. Conclusion

Oligomer of styrene and maleic anhydride synthesized by RAFT copolymerization (SMA-RAFT) was used to construct a novel strategy for nanoencapsulation via interfacially confined controlled/living radical miniemulsion polymerization. The hydrophilicity of ammonolyzed SMA-RAFT agent, SMA-RAFT agent structures, and adding the co-surfactant SDS were investigated, focusing on their influence on the particle morphology in the final latex. The following conclusions are drawn:

(1) The hydrophilicity of ammonolyzed SMA-RAFT agent tuned by the ammonolyzed/hydrolyzed degree or structures of the SMA-RAFT agents plays a key role in the final morphology where no co-surfactant was used. For SMA-RAFT1 with the alternative sequence structure, when the molar ratio of ammonia to anhydride groups is 0.9, most of the particles have a well-defined core–shell structure. When the ammonia dosage is too low (the molar ratio of ammonia to anhydride groups is 0.3) or too high (the molar ratio of ammonia to anhydride groups is 2.0), a large number of solid particles appear, co-existing with the nanocapsules. When the SMA-RAFT agent is fully ammonolyzed, the formation of the solid particles can be suppressed by extending chain length of SMA-RAFT1. However, SMA-RAFT3, which has the highest molecular weight and is most hydrophobic, turns out to be low efficient in encapsulation.
(2) Adding 0.5 wt% SDS and lowering the ammonia/anhydride group ratio significantly improved encapsulation efficiency. With such a strategy, the nanocapsules of well-defined core–shell structure can be achieved with very few solid particles by using SMA-RAFT1 and SMA-RAFT2.

We presented a novel technique for nanoencapsulation of liquid active substance. The technique is flexible in tuning polymer shell properties via RAFT polymerization chemistry. Anhydride groups incorporated in capsule surface offers great opportunities to functionalize the surface properties of the capsules. On the other hand, the technique is highly efficient, environmentally benign, robust, and scalable-up.

Acknowledgment

This work is financially supported by NSFC under Grant Nos. 20474057 and 20204015 and Program for New Century Excellent Talent in University.

References

[1] Caruso F, Caruso RA, Mohwald H. Science 1998;282:1111.
[2] Thurmond KB, Kowalewski T, Wooley KL. J Am Chem Soc 1997;119:6656.
[3] Wendland MS, Zimmerman SC. J Am Chem Soc 1999;121:1389.
[4] Werne T, Patten TE. J Am Chem Soc 1999;121:7409.
[5] Willert M, Rothe R, Landfester K, Antonietti M. Chem Mater 2001;13:3681.
[6] Ramirez LP, Landfester K. Macromol Chem Phys 2003;204:22.
[7] Tiarks F, Landfester K, Antonietti M. Macromol Chem Phys 2001;202:51.
[8] Landfester K, Rothe R, Antonietti M. Macromolecules 2002;35:1658.
[9] Tiarks F, Landfester K, Antonietti M. Langmuir 2001;17:908.
[10] Luo YW, Zhou XD. J Polym Sci Part A Polym Chem 2004;42:2145.
[11] Lelu S, Novat C, Graillat C, Guyot A, Bourgeat-Lami E. Polym Int 2003;52:542.
[12] Chern CS, Chen TJ, Liou YC. Polymer 1998;39:3767.
[13] Schork FJ, Luo YW, Smulders W, Russum JP, Butte A, Fontenot K. Adv Polym Sci 2005;175:129.
[14] Tsavalas JG, Schork FJ, de Brouwer H, Monteiro MJ. Macromolecules 2001;34:3938.
[15] Yang L, Luo YW, Li BG. Acta Polym Sinica 2004;3:462.
[16] Yang L, Luo YW, Li BG. J Polym Sci Part A Polym Chem 2005;43:4972.
[17] Luo YW, Liu XZ. J Polym Sci Part A Polym Chem 2004;42:6248.
[18] Vosloo JJ, De Wet-Roos D, Tonge MP, Sanderson RD. Macromolecules 2002;35:4894.
[19] de Brouwer H, Tsavalas JG, Schork FJ, Monteiro MJ. Macromolecules 2000;33:9239.
[20] Bon SAF, Bosveld M, Klumperman B, German AL. Macromolecules 1997;30:324.
[21] Tonge MP, McLeary JB, Vosloo JJ, Sanderson RD. Macromol Symp 2003;193:289.
[22] Luo YW, Tsavalas J, Schork FJ. Macromolecules 2001;34:5501.
[23] Butte A, Storti G, Morbidelli M. Macromolecules 2001;34:5885.
[24] Lansalot M, Davis TP, Heuts JPA. Macromolecules 2002;35:7582.
[25] Smulders W, Monteiro MJ. Macromolecules 2004;37:4474.
[26] Monteiro MJ, de Barbeyrac J. Macromolecules 2001;34:4416.
[27] Luo YW, Gu HY. Macromol Rapid Commun 2006;27:21.
[28] Quinn JF, Davis TP, Rizzardo E. Chem Commun 2001;11:1044.
[29] de Brouwer HD, Schellekens MA, Klumperman B, Monteiro MJ, German AL. J Polym Sci Part A Polym Chem 2000;38:3596.
[30] Zhu MQ, Wei LH, Li M, Jiang L, Du FS, Li ZC, et al. Chem Commun 2001;4:365.
[31] Bayer T, Eichhorn KJ, Grundke K, Jacobasch HJ. Macromol Chem Phys 1999;200:852.
[32] Hinnerk GB, Gudrun SN. Chem Eng Technol 2002;25:37.
[33] Chapman CB, Valentine L. J Polym Sci 1959;34:319.
[34] Bamford CH, Barb WG. Discuss Faraday Soc 1953;14:208.
[35] Hao XJ, Stenzel MH, Barner-Kowollik C, Davis TP, Evans E. Polymer 2004;45:7401.
[36] Davies MC, Dawkins JV, Hourston DJ. Polymer 2005;46:1739.
[37] Harrisson S, Wolley KL. Chem Commun 2005;26:3259.
[38] Matahwa H, McLeary JB, Sanderson RD. J Polym Sci Part A Polym Chem 2006;44:427.
[39] Hill DJT, O'Donnell JH, O'Sullivan PW. Macromolecules 1985;18:9.
[40] Garnier G, Duskova-Smrckova M, Vyhnalkova R, van de Ven TGM, Revol JF. Langmuir 2000;16:3757.
[41] Coleman LE, Bork JF, Dunn Jr H. J Org Chem 1959;24:135.
[42] Maxwell IA, Morrison BR, Napper DH, Gilbert RG. Macromolecules 1991;24:1629.
[43] Beuermann S, Buback M, Davis TP, Gilbert RG, Hutchinson RA, Olaj OF, et al. Macromol Chem Phys 1997;198:1545.

[44] Griffiths MC, Strauch J, Monteiro MJ, Gilbert RG. Macromolecules 1998;31:7835.
[45] Heuts JPA, Gilbert RG, Radom L. Macromolecules 1995;28:8771.
[46] Olaj OF, Vana P, Zoder M, Kornherr A, Zifferer G. Macromol Rapid Commun 2000;21:913.
[47] Albertin L, Stenzel MH, Barner-Kowollik C, Davis TP. Polymer 2006; 47:1011.
[48] Baussard JF, Habib-Jiwan JL, Laschewsky A, Mertoglu M, Storsberg J. Polymer 2004;45:3615.
[49] Vana P, Albertin L, Barner L, Davis TP, Barner-Kowollik C. J Polym Sci Part A Polym Chem 2002;40:4032.
[50] Smulders WW, Jones CW, Schork FJ. Macromolecules 2004;37:9345.
[51] Yang L, Luo YW, Li BG. Polymer 2006;47:751.
[52] Asua JM. Prog Polym Sci 2002;27:1283.